Beam coupling in 2×2waveguide arrays in fused silica fabricated by femtosecond laser pulses

Hongyun Chen[1], Xianfeng Chen[1]*, Yuxing Xia[1], Dayong Liu[2], Yan Li[2], and Qihuang Gong[2]

[1]*Department of Physics, Shanghai Jiao Tong University, 800 Dongchuan Road, Shanghai 200240, China*
[2]*State Key Laboratory for Mesoscopic Physics, Department of Physics, Peking University, Beijing 100871, China*
*xfchen@sjtu.edu.cn

Abstract: We demonstrate the coupling of a 2×2 waveguide array produced by a femtosecond laser in fused silica. The coupling constants of the waveguide array are obtained by measuring the ratio of output power of each waveguide by the coupled-mode theory. The variation of the coupled power between four waveguides as a function of the propagation distance is investigated experimentally and theoretically.

OCIS codes: (140.3390) Laser material processing; (140.7090) Ultrafast lasers; (230.7370) Waveguides.

References and links

1. K. M. Davis, K. Miura, N. Sugimoto, and K. Hirao, "Writing waveguides in glass with a femtosecond laser," Opt. Lett. **21**, 1729-1731 (1996).
2. K. Miura, J. Qiu, H. Inouye, T. Mitsuyu, and K. Hirao, "Photowritten optical waveguides in various glasses with ultrashort pulse laser," Appl. Phys. Lett. **71**, 3329-3331 (1997).
3. C. B. Schaffer, A. Brodeur, J. F. Garcia, and E. Mazur, "Micromachining bulk glass by use of femtosecond laser pulses with nanojoule energy," Opt. Lett. **26**, 93-95 (2001).
4. D. Liu, Y. Li, R. An, Y. Dou, H. Yang, and Q. Gong, "Influence of focusing depth on the microfabrication of waveguides inside silica glass by femtosecond laser direct writing," Appl. Phys. A. **84**, 257–260 (2006).
5. T. Pertsch, U. Peschel, F. Lederer, J. Burghoff, M. Will, S. Nolte, and A. Tünnermann, Opt. Lett. **29**,468 (2004).
6. D. Homoelle, S. Wielandy, A. L. Gaeta, N. F. Borrelli, and C. Smith, "Infrared photosensitivity in silica glasses exposes to femtosecond laser pulses," Opt. Lett. **24**, 1311-1313 (1999).
7. A. M. Streltsov and N. F. Borrelli, "Fabrication and analysis of a directional coupler written in glass by nanojoule femtosecond laser pulses," Opt. Lett. **26**, 42-43 (2001).
8. K. Minoshima, A. M. Kowalevicz, I. Hartl, E. P. Ippen, and J. G. Fujimoto, "Photonic device fabrication in glass by use of nonlinear materials processing with a femtosecond laser oscillator," Opt. Lett. **26**, 1516-1518 (2001).
9. W. Watanabe, T. Asano, K. Yamada, K. Itoh, and J. Nishii, "Wavelength division with three-dimensional couplers fabricated by filamentation of femtosecond laser pulses," Opt.Lett. **28**, 2491-2493 (2003).
10. Y. Kondo, K. Nouchi, T. Mitsuyu, M. Watanabe, P. G. Kazansky, and K. Hirao, "Fabrication of long-period fiber gratings by focused irradiation of infrared femtosecond laser pulses," Opt. Lett. **24**, 646-648 (1999).
11. E. N. Glezer, M. Milosavljevic, L. Huang, R. J. Finlay, T.-H. Her, J. P. Callan and E. Mazur, "Three-dimensional optical storage inside transparent materials," Opt. Lett. **21**, 2023 (1996).
12. E. N. Glezer and E. Mazur, "Ultrafast-laser driven micro-explosions in transparent materials," Appl. Phys. Lett. **71**, 882 (1997).
13. W. Watanabe, T. Toma, K. Yamada, J. Nishii, K. Hayashi and K. Itoh, "Optical seizing and merging of voids in silica glass with infrared femtosecond laser pulses," Opt. Lett. **25**, 1669 (2000).
14. W. Watanabe and K. Itoh, "Motion of bubble in solid by femtosecond laser pulses," Opt. Express. **10**, 603 (2002).
15. A. Szameit, D. Blomer, J. Burghoff, T. Pertsch, S. Nolte, and A. Tunnermann, "Hexagonal waveguide arrays written with fs-laser pulses", Appl. Phys. B: Lasers Opt. **82**, 507 (2006).
16. A. Szameit, J. Burghoff, T. Pertsch, S. Nolte, A. Tünnermann, and F. Lederer, "Two-dimensional solitons in cubic fs laser written waveguide arrays in fused silica," Opt. Express. **14**, 6055 (2006).
17. B. C. Stuart, M. D. Feit, S. Herman, A. M. Rubenchik, B. W. Shore, and M. D. Perry, "Optical ablation by high-power short-pulse lasers," J. Opt. Soc. Am. B **13**, 459 (1996).

18. M. Lenzner, J. Krueger, S. Sartania, Z. Cheng, Ch. Spielmann, G. Mourou, W. Kautek, and F. Krausz, "Femtosecond Optical Breakdown in Dielectrics," Phys. Rev. Lett. **80**, 4076 (1998).

1. Introduction

Many researchers have investigated the interaction of intense femtosecond laser pulses with a wide variety of materials. Structural modification both of the surface and inside the bulk of transparent materials has been demonstrated. By focusing ultrashort laser pulses inside optical transparent materials a localized and permanent increase of the refractive index can be achieved. When the sample is moved with respect to the laser beam a refractive index profile like in a buried waveguide can be produced. A variety of devices in glasses such as waveguides [1-5], couplers [6-9], gratings [10], and binary storages [11-14] have been demonstrated. The fabrication of photonic devices is based on nonlinear absorption around the focal volume of femtosecond laser pulses. Combination of multiphoton absorption and avalanche ionization allows one to deposit energy in a small volume of the material surrounding the focus, creating hot electron plasma; by a mechanism that is still under investigation, transfer of the plasma energy to the lattice generates a local increase of the refractive index. In contrast to the conventional techniques this method can be applied to practically all transparent materials and offers the opportunity to produce two-dimensional waveguide arrays, and these arrays can be served as two-dimensional integrated photonic devices in communication systems. In order to utilize the two-dimensional waveguide arrays fabricated by femtosecond laser pulses for future applications, many researchers not only have studied their linear characters [5, 15] but also the nonlinear characters [16].

In this paper we have presented and characterized a 2×2 waveguide array produced by a femtosecond laser in fused silica, including cross-sectional image of the waveguide area by optical microscope and the correlative analysis. We provide a detailed characterization and description of the waveguide arrays and study the variation of the coupled power between four waveguides as a function of the propagation distance by the coupled-mode theory, these results can provide the basis for future applications for two-dimensional integrated optical devices.

2. Experiment on waveguide formation

For the fabrication of the waveguide arrays we used an amplified Ti:sapphire laser system with a central wavelength of 800 nm, a repetition rate of 1 kHz, an on-target pulse energy of 350 nJ and a pulse duration of about 120 fs. The sample was mounted upon a computer-controlled three-axis positioning system. The laser pulses were focused into a polished fused-silica sample by a long working distance 50× microscope objective with a numerical aperture of 0.5. The focal plane inside the sample was about $1500\,\mu m$ ~$1480\,\mu m$ deep. We wrote each waveguide along the x direction at the speed of $50\,\mu m/s$ for 4 times. A schematic of the setup is given in Fig. 1 and the microscopic image of the end facet of the sample is shown as the inset. The 2×2 waveguide array was fabricated with waveguide to waveguide spacing (measured from center to center) of $20\,\mu m$. The length of the end facet of waveguide was measured about $14\,\mu m$ in the z direction, while the width was about $4\,\mu m$ in the y direction. The minimum spacing between waveguides using this technique is determined by the longer length of the end facet of waveguide, which can be reduced to ~ $10\,\mu m$ by compensation for the focusing aberration. In order to characterize the refractive index change and the propagation loss of our waveguides, a 5 mm long waveguide was written. The refractive index change Δn of the waveguide was estimated to be $2.47\times10^{-3}\pm20\%$ by a nondestructive method [4]. And the propagation loss of the waveguide was measured to be ~0.56dB/cm at 632.8 nm.
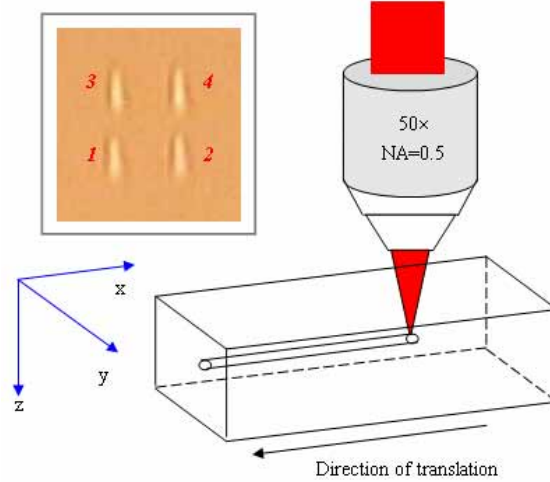
Fig. 1. Scheme of the writing process in transparent bulk material using fs laser pulses. Inset: Microscopic image of the end facet of the sample of the 2×2 waveguide array marked in Arabic numerals. The waveguide to waveguide spacing is 20 μm .

3. Results and discussion

From the microscopic image of the end facet of waveguide array given as the inset in Fig. 1, it can be seen that the cross-sectional profile shows an elliptical shape. The formation of this shape is possibly due to two causes. The first is that longitudinal intensity distribution of a Gaussian beam focused by an objective lens with NA of 0.5 has a Rayleigh distance much larger than its beam waist. The second reason is that formation of spherical aberration resulting from both the objective lens itself and the refraction at the interface between the air and the fused silica substrate makes the practical longitudinal size of the focal point much longer. In order to understand the refractive index profile better, we compared the cross section of the waveguide of the experimental results with that calculated by numerical simulation. For low-repetition-rate (1-100-kHz) systems the local index gradient is produced by a single pulse, and cumulative effects can be neglected. Therefore, since the material modification is due to energy transfer from the free electrons to the lattice, the size and shape of the material volume modified by the femtosecond pulse can be, to a first approximation, assumed to be equal to those of the region in which free electrons are generated. The evolution of the free-electron density, $\rho(t)$, in a medium exposed to an intense laser pulse can be described by the following rate equation [17, 18]

$$d\rho / dt = \alpha I(t)\rho(t) + \sigma_k I^k(t) \tag{1}$$

where α is the avalanche coefficient, which is $4cm^2/J$ [18] for fused silica, $\sigma_k = 6\times10^8 cm^{-3} ps^{-1}(cm^2/TW)^6$ [18] is the k-photon absorption coefficient , $k = Int(\Delta E / \hbar\omega + 1)$ is the number of absorbed photons, $\hbar$ is the Planck's constant, ω is the laser frequency, and the function $Int(x)$ yields the integer part of x. For an elliptical Gaussian beam, the intensity distribution near the focal spot can be expressed as

$$I(x,y,z,t) = I_0(\omega_0 / \omega(z))^2 \exp[-2(x^2+y^2)/\omega(z)^2]\exp[-(t/\tau_p)^2] , \tag{2}$$

Where ω_0 is the beam waist, $\omega(z) = \omega_0\sqrt{1+(z/z_0)^2}$, $z_0 = n\pi\omega_0/\lambda$ is the corresponding Rayleigh length, n is the refractive index, λ is laser wavelength. By solving Eq. (1) at

different points in the focal volume and plotting the asymptotic value $\rho(\infty)$ as a function of x, y and z, one can obtain a map of the free-electron density generated inside the material. We present the electron density profile in the y-z plane for waveguides written along the x direction, calculated with the parameters of the Gaussian beam ($\lambda = 0.8\mu m$) with pulse energy of $0.35\,\mu J$ focused to a waist of $\omega_0 = 3\mu m$. The contour plots of simulated electron density profiles near the focus point in the plane of x=0 is shown in Fig. 2. The cross-sectional image shown in inset of Fig. 1 is accordant with the computer simulation result.
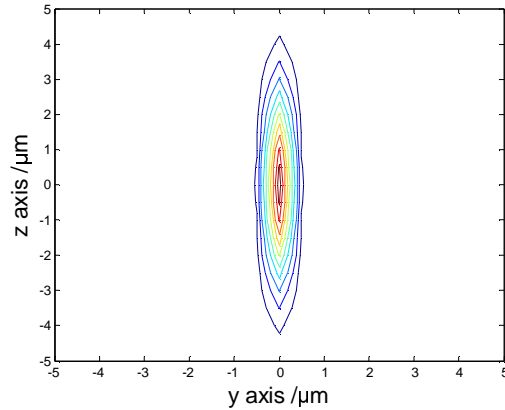
Fig. 2. Contour plots of simulated electron density profiles.

In order to analyze the guiding properties of the waveguide array, a He-Ne laser at 632.8nm was used. The input power was small so that the nonlinear effects can be neglected. The light was coupled into only one waveguide with a 10× microscope objective (NA=0.25), coupled out by a 20× objective and projected onto a CCD-camera. A schematic diagram of the setup is shown in Fig. 3. The intensity distributions at the output facet of the 2×2 waveguide array are displayed for different positions of the input beam in Fig. 4.
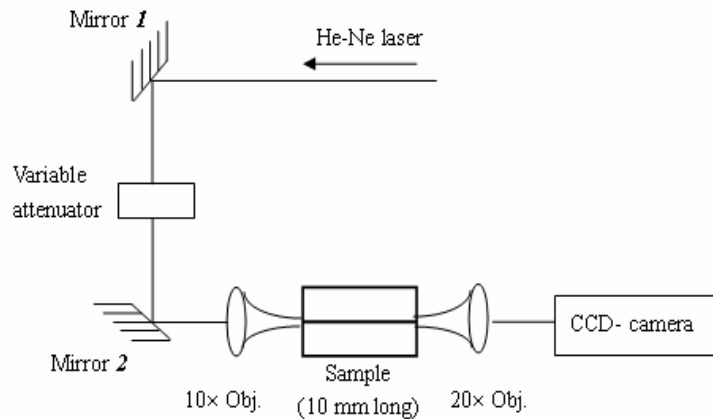
Fig. 3. Experiment setup for the investigation of output intensity distribution
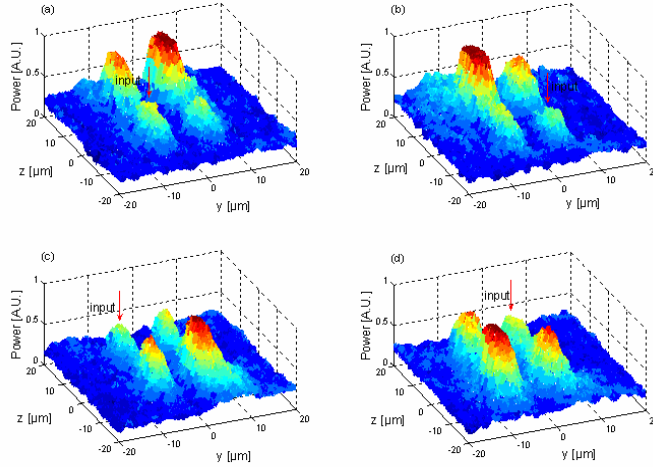
Fig. 4. Output intensity distribution for excitation of different waveguides of a 2×2 waveguide array

   To model the optical responses of the arrays we have used a coupled-mode approach and by considering only the nearest waveguides coupling. If the waveguides are marked in Arabic numerals as inset in Fig. 1, the amplitudes $a_m(x)$ (m=1, 2, 3, 4) of the electric fields propagating in the waveguides obey the following equations

$$\begin{cases} i\dfrac{da_1}{dx}+c_h a_2 +c_v a_3 +i\gamma|a_1|^2 a_1 = 0 \\[2mm] i\dfrac{da_2}{dx}+c_h a_1 +c_v a_4 +i\gamma|a_2|^2 a_2 = 0 \\[2mm] i\dfrac{da_3}{dx}+c_h a_4 +c_v a_1 +i\gamma|a_3|^2 a_3 = 0 \\[2mm] i\dfrac{da_4}{dx}+c_h a_3 +c_v a_2 +i\gamma|a_4|^2 a_4 = 0 \end{cases} \tag{3}$$

The coupling between adjacent guides induces the transverse dynamics. Energy exchange is caused by the overlap of the evanescent tails of the guided modes, which enter into Eq. (3) through coupling constants c_h, c_v for the horizontal, vertical directions, respectively. The last term describes the nonlinear Kerr effect, with a coefficient γ. At low powers, the nonlinear term of Eq. (3) can be ignored, the ordinary differential equation is then analytically integrable. If the first waveguide is excited with unit power, the solution of the Eq. (3) is

$$\begin{cases} a_1 = \cos(c_h x)\cos(c_v x) \\ a_2 = i\sin(c_h x)\cos(c_v x) \\ a_3 = i\cos(c_h x)\sin(c_v x) \\ a_4 = -\sin(c_h x)\sin(c_v x) \end{cases} \tag{4}$$

Thus, the output powers of the four waveguide, $P(x)=a^*(x)a(x)$, after propagation through the waveguide arrays are:

$$P_1(x)=\cos^2(c_h x)\cos^2(c_v x), \quad P_2(x)=\sin^2(c_h x)\cos^2(c_v x),$$

$$P_3(x)=\cos^2(c_h x)\sin^2(c_v x), \quad P_4(x)=\sin^2(c_h x)\sin^2(c_v x), \tag{5}$$

The ratio of the output power of waveguide is measured as follows:

$$P_3(x)/P_1(x) = \sin^2(c_v x)/\cos^2(c_v x) = 1.448 ,$$

$$P_4(x)/P_3(x) = \sin^2(c_h x)/\cos^2(c_h x) = 1.309 , \tag{6}$$

The sample is 10-mm long, thus the coupling coefficients $c_h = 0.853 cm^{-1}$, $c_v = 0.877 cm^{-1}$ can be obtained. The coupling constants are achieved by the ratio of output power of each waveguide. This method is different from that in the Ref. [5]. Moreover, the coupling in the horizontal and vertical directions is almost equal, even though the image profile of waveguide shows high asymmetry as shown in the inset of Fig. 1. The reason for this unexpected behavior is that the different rates of decay of the evanescent field of the guided mode in the two orthogonal directions. The mode is broader and decays faster along the vertical direction, while along the horizontal direction the mode is narrow and decays slowly. Consequently, the overlap integral between the modes in the horizontal and vertical directions can be matched. In order to visualize how the intensity of the four waveguides varies, the relation of power and the propagation distance is plotted by numerical method. Figure 5 shows the output power of each waveguide as a function of propagation distance x when the waveguide marked Arabic numeral 1 was excited. It can be clearly seen that the output power of the initial excited waveguide becomes minimal when the beams propagating 10mm, while the output power of the diagonal waveguide marked Arabic numeral 4 becomes maximal. The splitting ratio is about 18:23:26:33 for the four waveguides, which is an important detail in the design of two-dimensional integrated optical devices. Furthermore, it can be seen that the output powers of waveguides numbered 2 and 3 should be equal if $c_h = c_v$ in Eq. (5), the difference between the

c_h and c_v may be due to the asymmetry of the waveguide which shape is nearly elliptical.
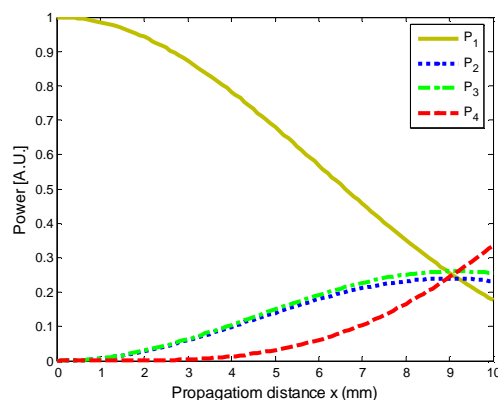
Fig. 5. The coupled powers of waveguide as a function of propagation distance x.

4. Conclusion

In conclusion we have demonstrated and characterized a 2×2 waveguide array produced by a femtosecond laser in fused silica. Using the coupled-mode theory, we calculated the coupling constants of the waveguide array through the ratio of output power of each waveguide and demonstrated the variation of coupled power in each waveguide as a function of the waveguide length. These results may pave the way for the realization of new applications using femtosecond nonlinear materials processing.

Acknowledgments